An experimental Bullard–von Kármán dynamo

2006 New J. Phys. 8 329

(http://iopscience.iop.org/1367-2630/8/12/329)

New Journal of Physics
The open-access journal for physics

An experimental Bullard–von Kármán dynamo

Mickael Bourgoin[1], Romain Volk[2], Nicolas Plihon[2], Pierre Augier[2], Philippe Odier[2] and Jean-François Pinton[2]

[1] Laboratoire des Écoulements Géophysiques et Industriels, CNRS UMR5519, BP53, 38041 Grenoble, France
[2] Laboratoire de Physique de l'École Normale Supérieure de Lyon, CNRS UMR5672, 46 Allée d'Italie, 69007 Lyon, France
E-mail: pinton@ens.lyon.fr

New Journal of Physics **8** (2006) 329
Received 25 October 2006
Published 21 December 2006
Online at http://www.njp.org/
doi:10.1088/1367-2630/8/12/329

Abstract. Inspired by a design originally proposed by Bullard (1955 *Proc. Camb. Phil. Soc.* **51** 744), we report a simple experimental arrangement which generates a turbulent fluid dynamo in the laboratory. It is based on a von Kármán gallium flow and it effectively models an 'alpha–omega' dynamo process, in which the alpha component is realized by external wirings, while the omega contribution fully incorporates the flow turbulence. In the dynamo state, we observe intermittent reversals of the dipole field, as well as excursions. The bifurcation develops through an 'on–off' regime.

Contents

PII: S1367-2630(06)35824-7

1. Introduction

The dynamo effect is believed to be at the origin of the magnetic field of planets and stars [2]. In this process, a fraction of the kinetic energy of motion of an electrically conducting fluid (liquid iron in the case of the Earth's core) is converted into magnetic energy. It is a nonlinear instability that occurs above a threshold, i.e. when the motion of the fluid is so vigorous that the stretching of magnetic field lines overcomes the Joule (resistive) dissipation. Not all fluid motions are appropriate. Anti-dynamo theorems invalidate large classes of flows, for instance two-dimensional motions [3]. Experimentally, the first observation was made in 1964 with solid rotor motions [4]. The turn of the century saw the advent of fluid dynamos with liquid sodium experiments in Karlsruhe [5], Riga [6], and recently VKS2 [7], operating in progressively less constrained geometries. One of the goals of experimental studies has been to generate a fully homogeneous dynamo. Solid rotor experiments [4] and later fluid experiments in Riga and Karlsruhe operated with homogenous electrical conditions but prescribed motions. In the experiment reported here, the opposite limit is explored. The flow is fully turbulent with very large fluctuations [8] but the current paths are partly imposed. As far as we know this limit has not been studied before experimentally.

A dynamo cycle can be viewed as a series of magnetic induction steps in which an initial magnetic seed field $\boldsymbol{B}_0$, transported and stretched by the velocity gradients in an electrically conducting flow, gives rise to an induced magnetic field component $\boldsymbol{B}_1$, which in turn generates an induced field $\boldsymbol{B}_2$, etc. until eventually the contribution after n steps $\boldsymbol{B}_n$ reinforces $\boldsymbol{B}_0$ [9]. If this feedback process is efficient enough, $\boldsymbol{B}_0$ is self-sustained (it is the neutral mode of the dynamo instability). For this to happen, studies to date have identified differential rotation and helical motions as key ingredients for the fluid motion. For instance, differential rotation (or zonal motions) can efficiently induce a toroidal magnetic field from a poloidal field [10]. The reciprocal conversion, i.e. the generation of a poloidal magnetic field from a toroidal one would complete the dynamo cycle. Helical motions in columns, present in several models of convection-driven dynamos in a sphere, have been shown to be able to achieve this [11, 12]. Helical flow geometries are interesting because they are able to induce currents locally parallel to the magnetic field [13, 14]. The Riga dynamo experiment [6] is based on an helical motion of the Ponomarenko type [15]. Organized arrays of helical motions in the spirit of the Roberts flow [16] drive the Karlsruhe dynamo experiment [5]. The mean field theory of magnetohydrodynamics [17] shows that if the turbulence is helical (or at least not parity-invariant) it may contribute to the conversion of a toroidal field into a poloidal one. The associated induction mechanism, usually called the alpha effect, is widely used and has been very successful for the development of astrophysical dynamo models [18]. However, for liquid metal flows in the laboratory, experiments have shown the contributions of small scale turbulent motions to be weak [19]–[21]. The actual role of turbulence and its positive or negative influence on the dynamo cycle is at present very much debated, and the study of a dynamo generated from a fully turbulent flow is of great interest. The recent VKS2 [7] findings are quite promising, but the experiment involves the complex operation of sodium flows.

We propose here a model that can be conveniently explored in the laboratory. Part of the dynamo cycle is generated by an external feed-back but the flow turbulence is included and has a leading role. That is, we relax the requirement that the current path be fully homogeneous, and we effectively prescribe the mechanism by which a toroidal magnetic field generates a poloidal one. However, the poloidal to toroidal conversion remains the result of a fully turbulent process.

2. Experimental set-up

Our experiments are carried out in the set-up sketched in figure 1. The flow is produced by the rotation of two disks inside a stainless steel cylindrical vessel filled with liquid gallium. The cylinder radius R is 97 mm and its length is 323 mm. The disks have a diameter equal to 165 mm and are fitted to a set of eight blades with height 10 mm. They are separated by a distance $H = 203$ mm. The disks are driven by two 11 kW AC-motors which provide a constant rotation rate in the interval $\Omega \in [0.5, 25]$ Hz with a stability of about 0.1%. The system is cooled by a water circulation located behind the driving disks; the experiments are made with the flow in a temperature interval between 42 and 48 °C. Liquid gallium has density $\rho = 6.09 \times 10^3\,\mathrm{kg\,m^{-3}}$, and electrical conductivity $\sigma = 3.68 \times 10^6\,\mathrm{ohm^{-1}\,m^{-1}}$, hence a magnetic diffusivity $\lambda = 1/\mu_0\sigma = 0.22\,\mathrm{m^2\,s^{-1}}$. Its kinematic viscosity is $\nu = 3.1 \times 10^{-7}\,\mathrm{m^2\,s^{-1}}$. The integral kinematic and magnetic Reynolds numbers are defined as $Re = 2\pi R^2\Omega/\nu$ and $R_\mathrm{m} = 2\pi R^2\Omega/\lambda$. Values of R_m up to five are achieved, with corresponding Re in excess of 10^6.

Magnetic induction measurements are performed using Hall sensor probes inserted into the flow in the mid plane, half way between the axis and the vessel wall. We measure the magnetic field component in the axial direction (B_z) and in the azimuthal direction (B_θ). Data are recorded using a National Instrument PXI-4472 digitizer at a rate of 1000 Hz with a 23 bit resolution.

The above set-up is used to build a simple laboratory dynamo, very much inspired by the solid rotor arrangement proposed by Sir Edward Bullard [1]. Consider the case when the two disks counter-rotate at the same rate Ω. When an axial magnetic field B_{0z} is applied (by imposing current in the external coils, as in figure 1(upper), the flow differential rotation induces a toroidal field $\boldsymbol{B}_\theta$. This can be seen from the induction equation

$$\frac{\partial \boldsymbol{B}}{\partial t} = \nabla \times (\mathbf{u} \times (\boldsymbol{B} + \boldsymbol{B}_0)) + \lambda \Delta \boldsymbol{B} \tag{1}$$

where $\mathbf{u}$ is the velocity in the flow. For a constant and uniform axial field applied, one obtains in the quasi-static limit at low magnetic Reynolds numbers [8, 19, 22],

$$0 \sim B_{0,z}\frac{\partial u_\theta}{\partial z} + \lambda \Delta B_\theta \tag{2}$$

so that the toroidal induced field is directly related to the differential rotation in the axial direction. This is the 'omega' induction mechanism. It is a linear effect, and the time average of the toroidal field at the measurement location verifies $B_\theta = kR_m B_{0,z}$, where k is a 'geometric' constant which in our experiment has been measured of the order of 0.1. However, due to the turbulent nature of the flow, the instantaneous values $B_\theta(t)$ have strong fluctuations: the standard deviation is of the order of the mean.

The poloidal to toroidal conversion is obtained when a signal linearly proportional to B_θ is used to drive the current source that feeds the coils, which, in turn, generate B_{0z} (figure 1(lower diagram)). As a result, $B_{0,z} = GB_\theta$ with G an adjustable gain. In this closed loop the average axial field obeys $B_z = GkR_mB_z$. A necessary condition for a self-sustained state is then $GkR_m = 1$. It corresponds to rotation rates of the disks larger than $\Omega^\mathrm{c} = \lambda/2\pi GkR^2$. Clearly, the adjustable gain of the linear amplifier allows us to set the value of Ω^c to an experimentally accessible range. At this point, it should be emphasized that although the feed-back scheme is very similar to the

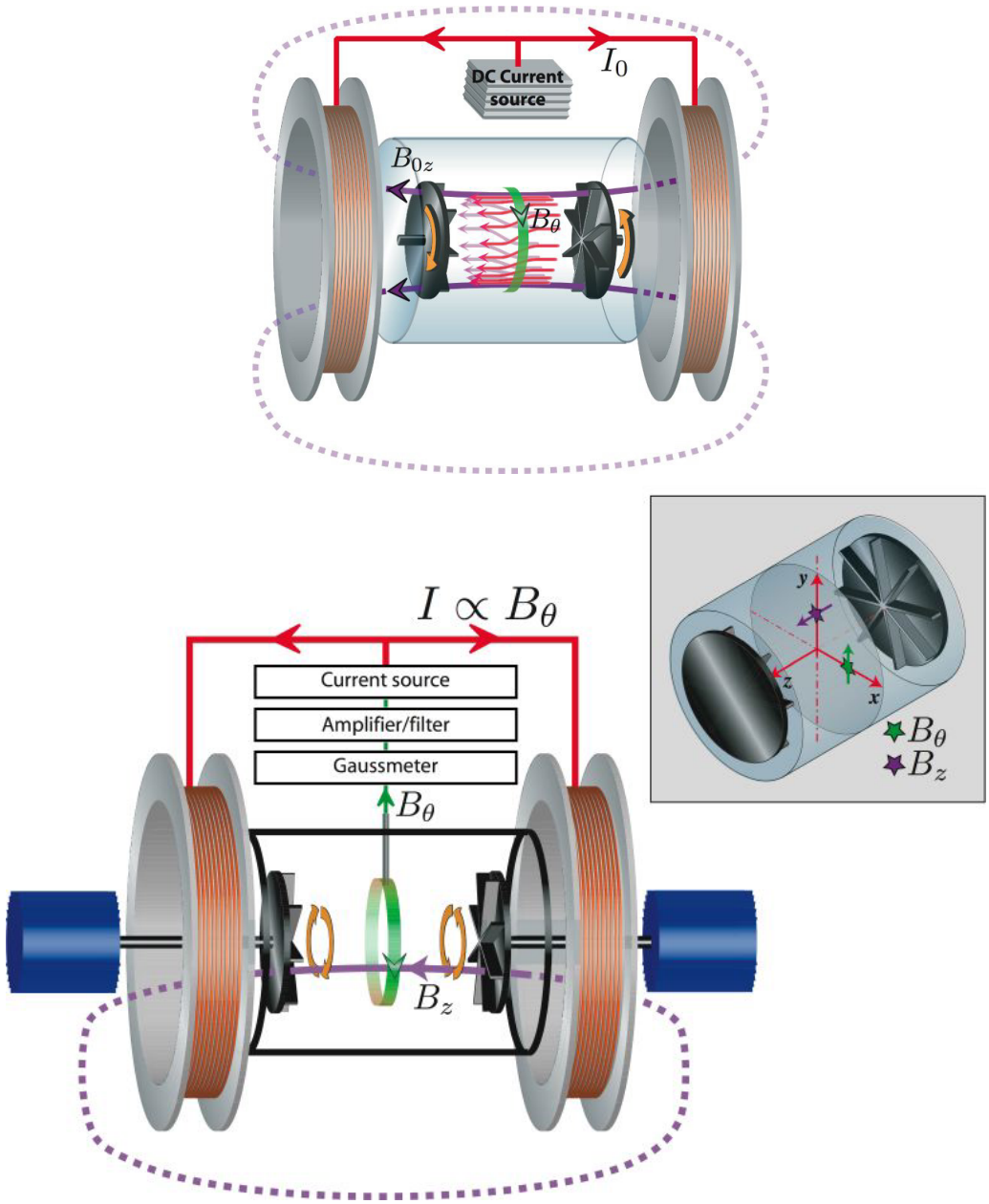

Figure 1. Experimental set-up: a von Kármán flow of liquid gallium is generated in a cylindrical vessel between two counter-rotating disks driven by two AC-motors. (Upper figure): omega effect; the differential rotation advects and stretches an externally applied axial field $B_{0,z}$ (red lines) so as to generate a toroidal component B_θ (green line). (Lower figure): positive toroidal to poloidal feed-back: the amplitude of B_θ is used to drive a power source which generates the current in the external loop. Two Helmholtz coils are set on either end of the cylindrical flow vessel. B_θ is measured in the mid-plane by a Hall probe connected to a Bell gaussmeter. Its value is fed into a linear amplifier whose output drives a Kepco BOP current source. The inset shows the actual position of the Hall probes used to measure the poloidal (B_z) and the toroidal (B_θ) magnetic fields inside the vessel; the probes are inserted into the flow at $R/2$ from the rotation axis.

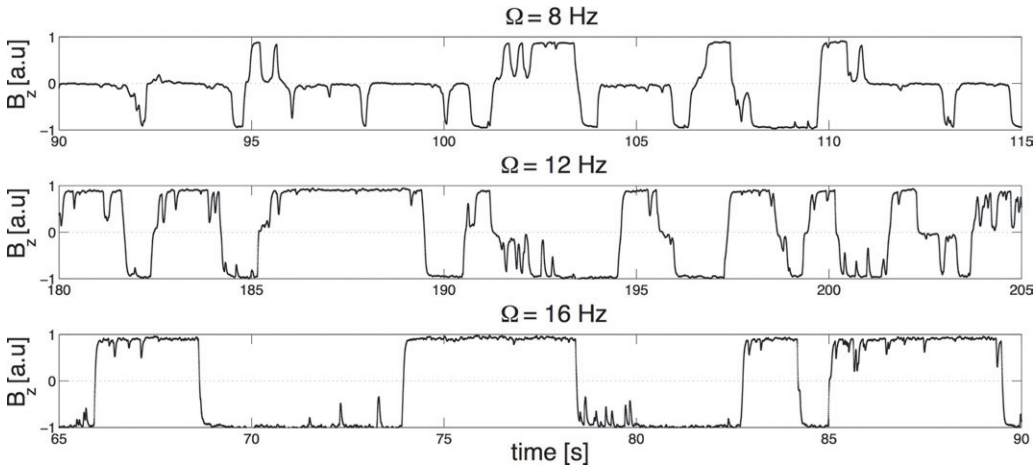

Figure 2. Evolution of the axial induced field B_z as a function of time, for three values of Ω. Saturated (maximum) values correspond to $B_{\rm sat} \sim \pm 30\,\mathrm{G}$. No external field is applied, other than the Earth's and its local distortion by the laboratory environment.

Bullard rotor dynamo [1, 23], it fully incorporates a fluid turbulence component—fluctuations up to 114% for the omega effect have been reported for this flow in [8]. The feed-back mechanism would lead to a stationary dynamo in the absence of these fluctuations, but in their presence one may expect richer dynamical regimes.

3. Results

3.1. Global features

Figure 2 shows the time evolution of the axial magnetic field (featuring the expected poloidal dynamo dipole) for different rotation rates of the disks. The current amplifier stage is set so that $\Omega^{\rm c} = 8.3$ Hz. In this section, we describe global characteristics of the magnetic behaviour of the system, and we shall return to specific points in the next sections.

Let us first consider the system behaviour as the rotation rate of the driving disks is progressively increased. The magnetic field is initially null at all times, save for the ambient Earth's field. It remains so until a sufficient rotation rate is reached. At this point, one observes the occurrence of intermittent bursts: the magnetic field grows spontaneously at irregular intervals, with either polarity. This corresponds to times when the fluctuations in the differential rotation reach a level high enough to satisfy the instability condition. In figure 2, it is the case when $\Omega = 8$ Hz: during these dynamo bursts, the magnetic field reaches a finite value $\pm B_{\rm sat}$, held for durations, $\langle T_{\rm burst}\rangle \Omega \sim 5$ on average (or $\langle T_{\rm burst}\rangle \lambda / R^2 \sim 10$ if one compares to the diffusion time of the magnetic field across the flow volume). The fact that either polarity is realized is due to the symmetry of the induction equation

$$\partial_t \boldsymbol{B} = \nabla \times (\mathbf{u} \times \boldsymbol{B}) + \lambda \Delta \boldsymbol{B} \tag{3}$$

which is invariant under the change $\boldsymbol{B} \to -\boldsymbol{B}$, with the velocity field $\mathbf{u}$ unchanged.

As the disks rotation rate is increased further, the dynamo bursts grow longer until a regime is reached when the magnetic field is always present, with either polarity. This is the case in figure 2, for the rotation rate $\Omega = 16$ Hz. The polarity of the field is not constant in time: the magnetic field spontaneously reverses its direction, at irregular time intervals. One also notes the occurrence of excursions, i.e. times when the magnetic field decreases as if about to reverse, but then returns to its initial value and polarity. This non-trivial dynamics results from the fluctuations due to the flow turbulence: the velocity fluctuations [8] together with the creation of a dynamo field induced in the presence of (non-independent) multiplicative and additive noise in the induction equation.

In our experiment, the value of the magnetic field at saturation $B_{\rm sat}$ is set by the maximum current that can be drawn from the power amplifier driving the current in the coils. We measure $B_{\rm sat} \sim 30$ G, a value such that the Lorentz forces cannot modify the hydrodynamic flow. The corresponding interaction parameter, computed as $N = \sigma B_{\rm sat}/\rho\Omega$, is of the order of 10^{-3}. The saturation of the instability is therefore driven by the nonlinearities in the feed-back loop (essentially the amplifier) rather than by the back-reaction of Lorentz forces on the dynamical velocity field. As a consequence, the B_z component of the dynamo field saturates at the same mean amplitude $B_{\rm sat}$ for all rotation rates; i.e. $B_{\rm sat}$ corresponds to the magnetic field generated by the coils when the current source is saturated. However, the saturation amplitude of the toroidal field, which includes the omega effect, increases linearly with Ω, $B_\theta = kR_m B_{\rm sat}$.

An interesting finding is that the presence of turbulent fluctuations plays a crucial role in the dynamics of the self-generated magnetic field, in particular for the triggering of reversals. In our set-up, the current source is driven by an amplifier whose input is $\bar{B}_\theta + g \cdot b'_\theta$, with $\bar{B}_\theta$ the low pass DC component of B_θ and b'_θ its AC fluctuating part. This arrangement allows us to study separately the role of slow variations and turbulent fluctuations in the feed-back loop. In all results reported here, we have set $g = 1.2$. A homopolar dynamo, without reversals, is obtained for smaller values of g. We have also observed that the dynamics is different when the b'_θ input in the amplifier is replaced by a synthetic Gaussian white noise. A full investigation of the role of noise in the development of the instability will be made in forthcoming studies.

In the arrangement reported here and shown in figure 1, the alpha effect is driven by the omega effect as evaluated by measurements from a single probe. We have verified that the dynamo behaviour is unchanged if the omega effect is integrated from measurements along a radius in the shear layer. This is because the magnetic field dyamics is strongly correlated (in space) in this flow [8], as the characteristic scale of magnetic diffusion $\ell_{\rm B} = \sqrt{\lambda/\Omega}$ is of the order of the cylinder radius.

3.2. Bifurcation

We describe in this section the onset of the dynamo instability. Since the magnetic field grows with either polarity with equal probability, its mean value is always equal to zero. We therefore compute and show in figure 3 the evolution of the variance of the axial field B_z as the rotation rate of the disks increases. For $\Omega < \Omega'^{\rm c} = 5.8$ Hz, the amplitude of fluctuations is almost null, while it grows abruptly for larger rotation rates. Close to this bifurcation, the variance $B^2_{\rm rms}$ grows approximately linearly with Ω, but then saturates for frequencies larger than about 10 Hz when the dynamo field is always on. This is due to the vanishing of the fraction of time when the axial magnetic field is zero, while its maximum value is set at $B_{\rm sat}$.

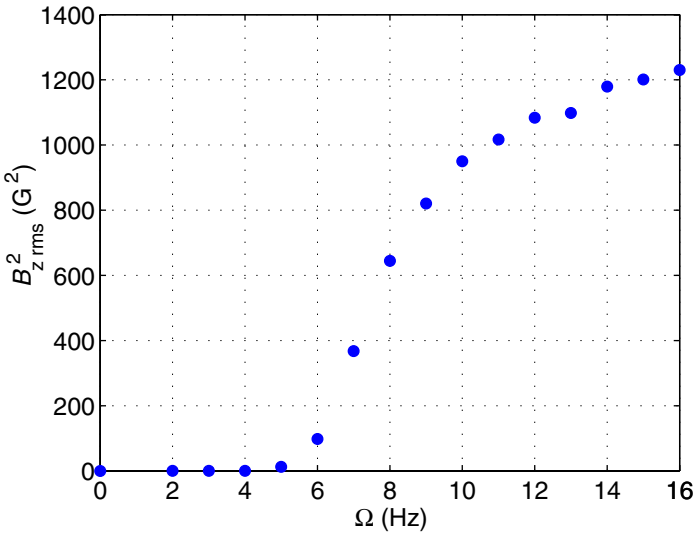

Figure 3. Evolution of the variance of the time fluctuations of the axial magnetic field, as the disks' counter-rotation rate is increased. Measurement is made in the mid-plane as shown in figure 1.

A noteworthy feature of the bifurcation, as can already by seen in figure 2, is that it proceeds via an 'on–off' regime. This is best evidenced in the changes of the probability density functions (PDFs), shown in figure 4. For low rotation rates, bursts of magnetic field are observed, but the maximum of the PDF is for $B_z = 0$. As the rotation rates is increased beyond the bifurcation threshold, the probability of measuring a zero magnetic field steadily decreases and the PDFs peak at $\pm B_{\mathrm{sat}}$. This scenario has been previously hypothesized for dynamo experiments and models [24]–[28]. It was not observed in the experiments in Riga [6], Karlsruhe [5] and VKS2 [7], for which the dynamo process is completely homogeneous.

Schematically, the magnetic field in our experiment has three possible states: zero and $\pm B_{\mathrm{sat}}$. The time spent in each state varies as the rotation rate of the disks is increased above threshold (see figure 5). The average duration τ_0 of the zero-state intervals, which in the intermittent 'on–off' transient coincides with the waiting time between bursts, rapidly drops while the average duration, τ_{sat}, of the saturated-state intervals (either $+B_{\mathrm{sat}}$ or $-B_{\mathrm{sat}}$), which in the fully developed regime coincides with the waiting time between two reversals, grows continuously up to the highest rotation rates we have run. The cross-over occurs around 9 Hz; for higher rotation rates the dynamo is always 'on' and spends most of the time in the saturated states and the zero-state contribution is mostly due to short events, called excursions, where the magnetic field briefly decreases in amplitude almost to zero before growing back with the same polarity (see subsection 3.3 below). Further studies are currently being done to explore regimes farther from the threshold in order to elucidate in particular if the average waiting time between reversals will continue to grow or if there is an asymptotic limit.

It is interesting to note that the actual threshold $\Omega'^{\mathrm{c}} = 5.8$ Hz at which the 'on–off' instability starts is lower than the threshold $\Omega^{\mathrm{c}} = 8.3$ Hz predicted from the gain G of the feed-back loop and from open loop measurements of k for the averaged omega effect (where only the averaged conversion of an externally applied stationary poloidal field $B_{0,z}$ into a toroidal one is considered, without caring about the turbulent fluctuations). The intermittent transient occurs for rotation

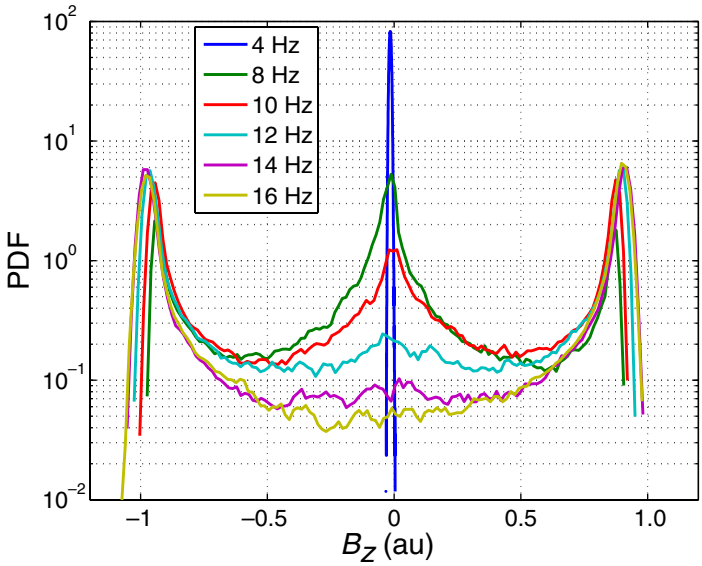

Figure 4. PDFs of B_z component, for increasing rotation rates. The most probable value is $Bz = 0$ up to and slightly over Ω'^{c}, but then the PDFs' maxima occur at $B_z = \pm B_{sat}$. Note that although the current in the coils is at its maximum value, the peaks of B_z change slightly with Ω because at the measurement point there is also a contribution due to the induction caused by the axial stretching of the magnetic field lines.

rates $\Omega'^{c} < \Omega < \Omega^{c}$, while the fully developed dynamo regime, where the magnetic field is almost always 'on', is observed for $\Omega > \Omega^{c}$. The transition between these two regimes is visible in figure 3 as a transition around Ω^{c} from a rapidly growing phase of B_{rms} to a saturation. This also coincides with a transition from PDFs of B_z with a dominant peak at $B_z = 0$ to PDFs with dominant peaks at $\pm B_{sat}$ occuring $\Omega \sim \Omega^{c}$, linked to the crossover between the τ_0 and τ_{sat} curves in figure 5.

3.3. Fully developed regime

We describe here the dynamical regime reached above the dynamo onset, when the dynamo is always 'on'. An example of the time dynamics of the axial field component is shown in figure 6 with a long time series progressively zoomed-in to detail reversals and excursions. In the mid-figure, one may note that during one polarity phase, the magnetic field can be quite steady as in the centre of the plot (e.g. $243 < t < 246$ s) or display larger fluctuations (e.g. $240 < t < 242$ s). In the latter case, the rotation rate is clearly above the instability onset but the turbulence induces strong fluctuations in the velocity gradients [8] and prevents the dynamo to set into a steady regime. In particular, there are times at which the instantaneous differential rotation decreases so significantly that the dynamo field decreases to zero. It may then either grow again with the same polarity or change its sign, producing either an excursion or a reversal.

As a result, magnetic field fluctuations occur over a wide range of timescales, from the long periods of quasi-steady polarity to rapid fluctuations. This is evidenced in the power spectrum of the complete time series shown in figure 7. In the higher frequency range (above the disks

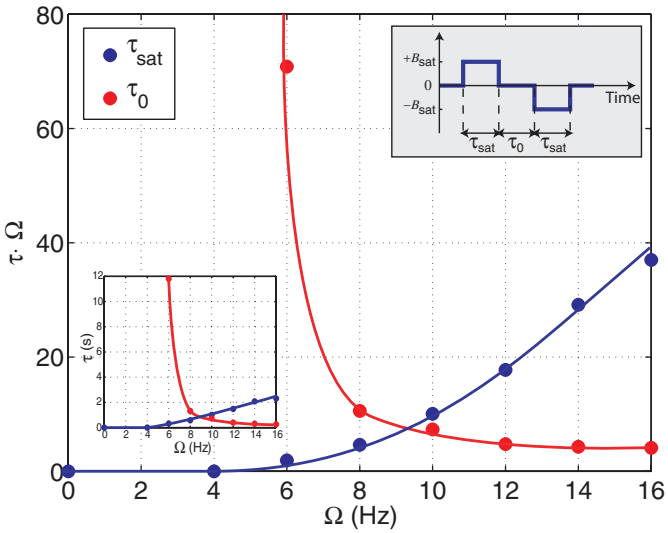

Figure 5. Evolution, with the disks rotation rate Ω, of the average duration of the intervals the dynamo spends in the zero state (red dots) and in the saturated states, either $+B_{\rm sat}$ or $-B_{\rm sat}$ (blue dots); the top right inset shows a schematic definition of these times. We have also checked that the average duration of $+B_{\rm sat}$ intervals is identical to the average duration of $-B_{\rm sat}$ intervals. The vertical duration axis has been normalized by the rotation rate Ω. The inset on the left bottom shows the same data with the vertical axis not normalized, i.e. with times directly expressed in seconds.

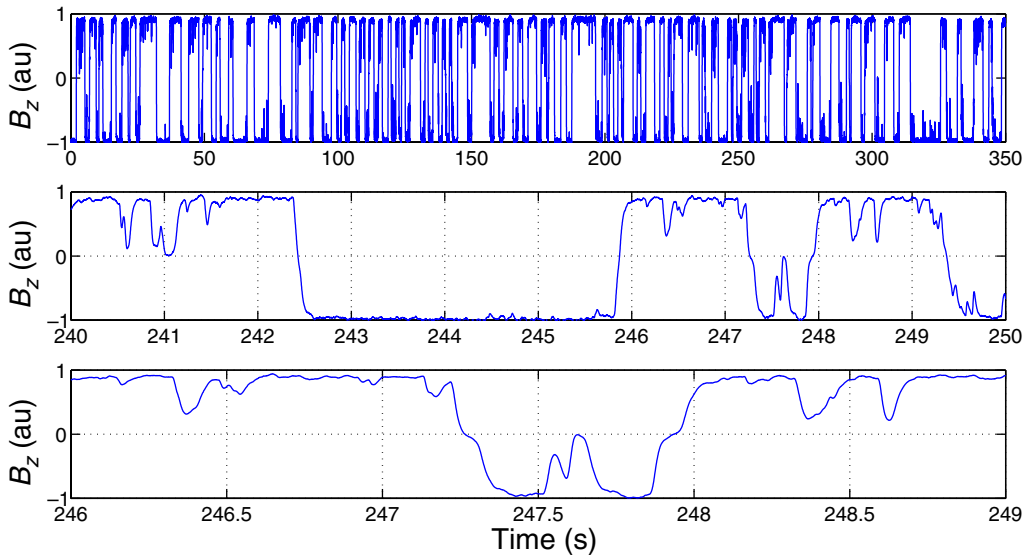

Figure 6. Example of dyamics of $B_z(t)$, at $\Omega = 16$ Hz. The evolution is zoomed from top to bottom. Magnetic field units are non-dimensionalized by $B_{\rm sat}$.

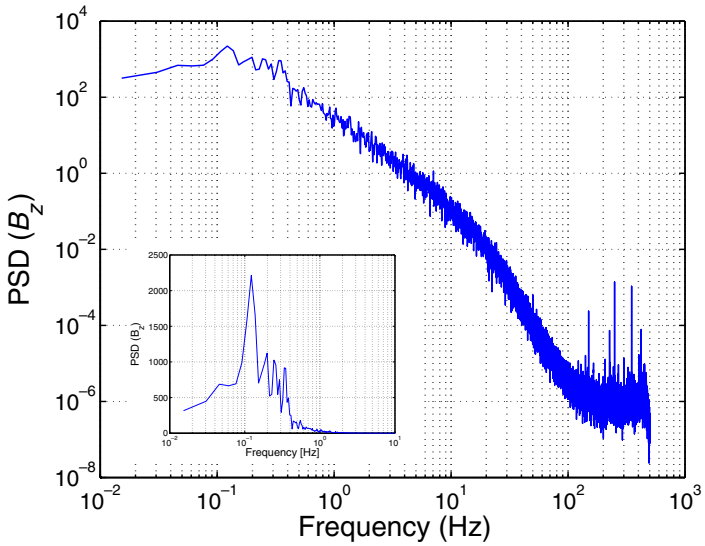

Figure 7. Spectrum of B_z component. $\Omega = 16$ Hz. The inset zooms on the low frequency part, with linear ordinates.

rotation rate), it is very similar to the spectrum of magnetic field induction from an externally applied field. The low frequency part is very wide and has a maximum around 0.16 Hz.

We have superimposed in figure 8 all 'down–up' reversals and the opposite of the 'up–down' reversals for the entire time series at $\Omega = 16$ Hz. Their shape is very robust with a characteristic reversal time of the order of 0.1 s, shorter than the mean duration of each polarity between reversals $\langle T^+ \rangle = \langle T^- \rangle = 2.3$ s, also widely distributed since their standard deviations ($T^+_{\rm rms} = T^-_{\rm rms} = 1.5$ s) are of the order of their mean. The values of the time intervals, and their fluctuations, are consistent with the broad peak in the lower frequency range of the signal power spectrum. For comparison, the magnetic diffusion time over the flow volume is of the order of $\tau_{\rm m} = R^2/\lambda = 0.05$ s, and the period of rotation of the disk is $1/\Omega = 0.06$ s. When the time axis is normalized by the rotation rate Ω, the mean profiles of the reversals collapse for all values of Ω (see inset of figure 8). This observation indicates that the reversal timescale is not related to a magnetic diffusion process but really to the system dynamics.

The probability density of the time interval between reversals ΔT is shown in figure 9. In agreement with the peak in the power spectrum, it has a most probable value of the order of 2.5 s. However, at large times the PDF of ΔT decays exponentially. This long time behaviour is consistent with a Poisson statistics, for which successive reversals would be independently triggered. However, the exact nature of the reversal dynamics remains to be elucidated. For instance, as one can see in figure 6, reversals occur with a dynamics such that the field variation slows down as its value approaches zero (times t around 247–248 s in the figure) or such that the field's time derivative remains high as the zero amplitude is crossed (times around 242.5 and 249.5 s). These different behaviours may result from generic characteristics for nonlinear systems driven by coupled additive and multiplicative noises (in the induction equation they come from the fluctuations in velocity and in the large scale dynamo field). But they could also be completely driven by the hydrodynamics of the von Kármán shear flow. Further experiments with different values of the feed-back gain G may help decide.

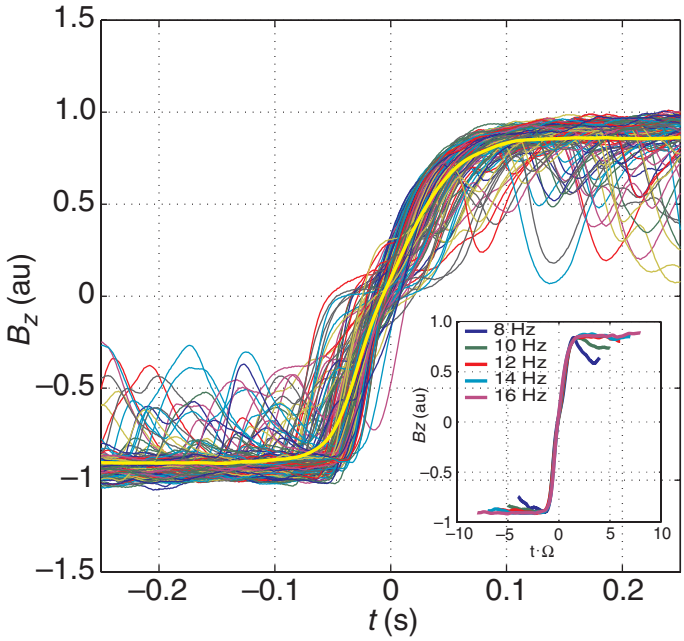

Figure 8. Superposition of all the reversals $-B_{\rm sat} \rightarrow +B_{\rm sat}$ and of the opposite of the reversals $+B_{\rm sat} \rightarrow -B_{\rm sat}$ for the entire time series at 16 Hz. The solid yellow line represents the profile averaged over all events. The inset shows the averaged profiles for different rotation rates Ω, with the time axis normalized by the corresponding value of Ω. Magnetic field units are non-dimensionalized by $B_{\rm sat}$.

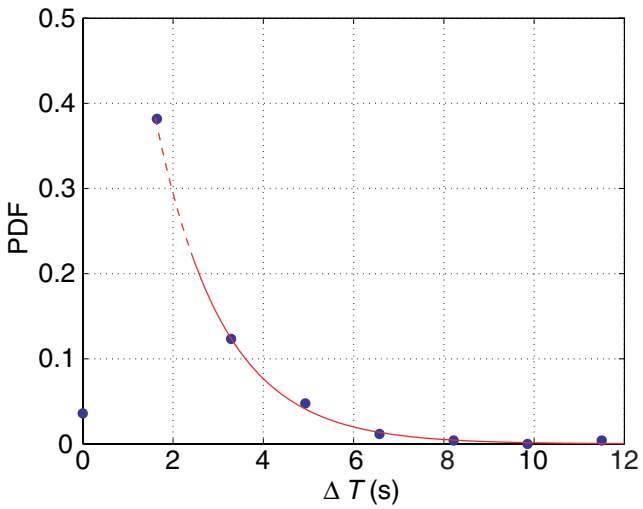

Figure 9. PDF of the time between reversals. The solid line is a decaying exponential fit on the last points.

Finally, we return to our estimation that due to the very low value of the interaction parameter, the magnetic field does not modify the dynamics of the gallium flow. We show in figure 10 (left panel) simultaneous recordings of the axial magnetic field and of pressure fluctuations at the flow wall. We find that the signals are uncorrelated (the maximum of the cross-correlation function

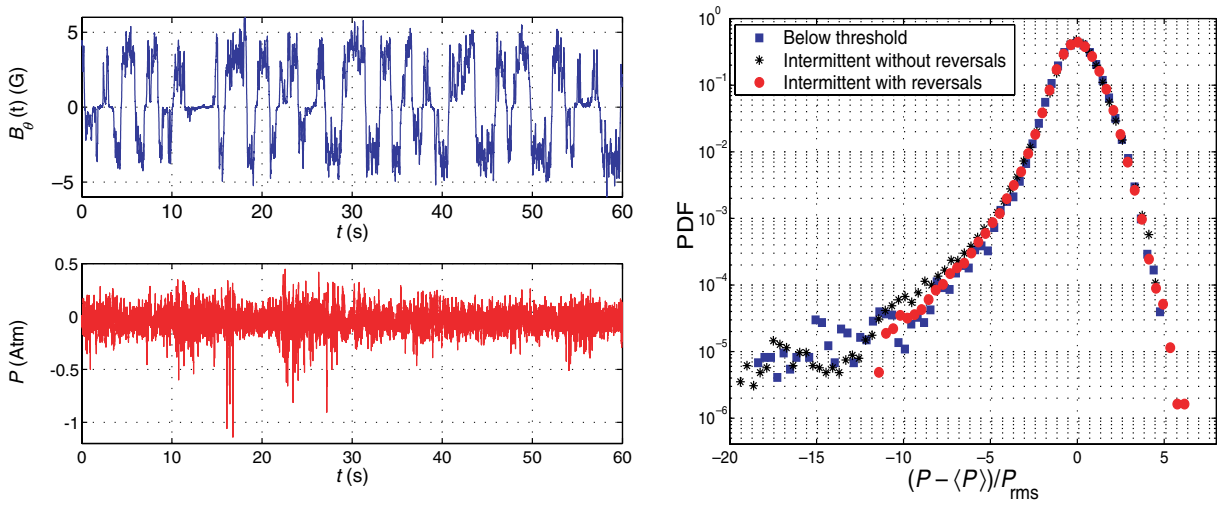

Figure 10. Pressure measurements, measured by a piezoelectric transducer mounted flush at the flow wall, at a distance 5 cm away from one of the driving disks (also about 5 cm off the mid-plane). (Left panel) magnetic field and pressure time series. The signals are not correlated; the amplitude of the cross-correlation function is below 10^{-2}. (Right panel) PDFs measured at 0.9 Ω^c and 1.2 Ω^c.

is below 10^{-2} at all times). On the right-hand side of the figure, we show the statistics of the pressure signal. It is unchanged below and above threshold and also whether the current source is unipolar (no reversal) or bipolar (with reversals).

4. Concluding remarks

We have reported here a convenient experiment in which some features of turbulent dynamos can be studied in a gallium laboratory experiment. Our arrangement models an 'alpha–omega' dynamo cycle, in which the 'omega' part is fully turbulent while the 'alpha' part is enforced by external wires. Even though the flow is fully turbulent the dynamo cycle operates and we observe a self-sustained field having the form of an axial dipole. We observe a dynamo bifurcation with reversals of the field, and equal probability for each polarity. These reversals are irregular in time, as in the dynamics of the Earth's field. In our set-up, they are induced by the turbulent fluctuations in the flow. The bifurcation proceeds via an 'on–off' regime. This behaviour and the nature of the bifurcation should be considered in the context of nonlinear instabilities in the presence of noise.

Several issues related to dynamo and nonlinear bifurcation can be addressed using the experimental arrangement reported here and will be explored in forthcoming studies:

1. The external gain in the feed-back loop amplifies induction effects. The effective magnetic Reynolds number in the system is then $R_m^{\text{eff}} = G R_m$. One consequence is that one can tune independently the magnetic Reynolds number and the kinetic Reynolds number of the flow. It will be interesting to analyse to which extend our arrangement provides a way to study MHD at varying magnetic Prandtl numbers (here defined as the ratio R_m/Re).

2. The use of a mean and a fluctuating component in the feed-back amplification stage provides a tool to study experimentally the role of fluctuations and noise in the bifurcation dynamics. Firstly, one can set the threshold by adjusting the gain of the feed-back loop so that one may choose to operate far above the dynamo onset. Secondly, several kinds of noise (coloured, correlated, etc) can be inserted into the feed-back loop, and the effects can be quantified. Some studies have shown that the dynamo threshold would be increased due to the presence of noise [28]–[30] while others suggested that small scale turbulence may not modify it or eventually help [31, 32]. The nature of the bifurcation may also change with the characteristics of the noise, particularly for the on–off regime [33].
3. One may also ask whether it is possible to synchronize the reversals by adding a periodic forcing (mechanical or applied field) in connection with stochastic resonance issues.
4. Finally, a promising possible development is the use of a current source such that the field at saturation is large enough for Lorentz forces to alter the flow. One of the open questions is how the field dynamics, including reversals, is changed in this case.

References

[1] Bullard E C 1955 The stability of a homopolar dynamo *Proc. Camb. Phil. Soc.* **51** 744
[2] Larmor J 1919 How could a rotating body such as the Sun become a magnet? *Rep. Brit. Assoc. Adv. Sci.* **159**
[3] Moffatt H K 1978 *Magnetic Field Generation in Electrically Conducting Fluids* (Cambridge: Cambridge University Press)
[4] Lowes F J and Wilkinson I 1963 Geomagnetic dynamo: a laboratory model *Nature* **198** 1158
Lowes F J, Wilkinson I 1968 Geomagnetic dynamo: an improved laboratory model *Nature* **219** 717
[5] Stieglitz R and Müller U 2001 Experimental demonstration of a homogeneous two-scale dynamo *Phys. Fluids* **13** 561
[6] Gailitis A *et al* 2000 Detection of a flow induced magnetic field eigenmode in the Riga dynamo facility *Phys. Rev. Lett.* **84** 4365
[7] Monchaux R *et al* 2006 Generation of magnetic field by a turbulent flow of liquid sodium *Phys. Rev. Lett.* in press
[8] Volk R, Odier P and Pinton J-F 2006 Fluctuation of magnetic induction in von Kármán swirling flows *Phys. Fluids* **18** 085105
[9] Bourgoin M, Odier P, Pinton J-F and Ricard Y 2004 An iterative study of time-independent induction effects in magnetohydrodynamics *Phys. Fluids* **16** 2529
[10] Roberts P H and Soward A M 1992 Dynamo theory *Ann. Rev. Fluid Mech.* **24** 459 (1992)
Cardin P, Brito D, Jault D, Nataf H-C and Masson J-P 2002 Towards a rapidly rotating liquid sodium dynamo experiment *Magnetohydrodynamics* **38** 177
[11] Busse F H 1978 Magnetohydrodynamics of the Earth's Dynamo *Ann. Rev. Fluid Mech.* **10** 435
[12] Volk R 2005 Contributions aux grandes échelles et fluctuations d'induction en magnétohydrodynamique, application à l'effet dynamo *PhD Thesis* École Normale Supérieure de Lyon
[13] Lehnert B 1957 An experiment on axisymmetric flow of liquid sodium in a magnetic field *Ark. Fys.* **13** 109
[14] Pétrélis F, Marié L, Bourgoin M, Chiffaudel A, Daviaud F, Fauve S, Odier P and Pinton J-F 2003 Non linear magnetic induction by helical motion in a liquid sodium turbulent flow *Phys. Rev. Lett.* **90** 174501
[15] Ponomarenko Yu B 1973 *J. Appl. Mech. Tech. Phys.* **14** 775
[16] Roberts G O 1972 *Phil. Trans. R. Soc.* A **271** 411–54
[17] Krause F and Rädler K-H 1980 *Mean Field Magnetohydrodynamics and Dynamo Theory* (New York: Pergamon)

[18] Beck, Brandenburg A, Moss D, Shukurov A and Sokoloff D 1996 Galactic magnetism: recent developments and perspectives *Ann. Rev. Astron. Astrophys.* **34** 155–206

[19] Bourgoin M, Volk R, Frick P, Kripchenko S, Odier P and Pinton J-F 2004 Induction mechanisms in von Kármán swirling flows of liquid gallium *Magnetohydrodynamics* **1** 13–31

[20] Volk R, Stepanov R, Denisov S, Frick P, Noskov V and Pinton J-F 2006 Induction, helicity and alpha effect in a toroidal screw flow of liquid gallium *Phys. Rev.* E **73** 046310

[21] Spence E J, Nornberg M D, Jacobson C M, Kendrick R D and Forest C B 2006 Observation of a turbulence-induced large scale magnetic field *Phys. Rev. Lett.* **96** 055002

[22] Odier P, Pinton J-F and Fauve S 1998 Advection of a magnetic field by a turbulent swirling flow *Phys. Rev.* E **58** 7397

[23] Rikitake T 1958 Oscillations of a system of disk dynamos *Proc. Camb. Phil. Soc.* **54** 89
Cook A E and Roberts P H 1970 The Rikitake two-disc dynamo system *Proc. Camb. Phil. Soc.* **68** 547

[24] Sweet D, Ott E, Finn J M, Antonsen T M Jr and Lathrop D P 2001 Blowout bifurcations and the onset of magnetic activity in turbulent dynamos *Phys. Rev.* E **63** 066211

[25] Nornberg M D, Spence E J, Kendrick R D, Jacobson C M and Forest C B 2006 Intermittent magnetic field excitation by a turbulent flow of liquid sodium *Phys. Rev. Lett.* **97** 044503

[26] Lozhkin S, Sokoloff D and Frick P 1999 Magnetic Prandtl number and the small-scale MHD-dynamo *Astron. Rep.* **43** (11) 753

[27] Leprovost N, Dubrulle B and Plunian F 2006 Intermittency in the homopolar disc-dynamo *Magnetohydrodynamics* **42** 131

[28] Laval J-P, Blaineau P, Leprovost N, Dubrulle B and Daviaud F 2006 Influence of turbulence on the dynamo threshold *Phys. Rev. Lett.* **96** 204503

[29] Schekochihin A A, Cowley S C, Maron J L and McWilliams J C 2004 Critical magnetic Prandtl number for small-scale dynamo *Phys. Rev. Lett.* **92** 054502

[30] Pétrélis F and Fauve S 2006 Inhibition of the dynamo effect by phase fluctuations *Europhys. Lett.* **75** (4) 602–8

[31] Ponty Y, Minnini P D, Montgomery D, Pinton J F, Politano H and Pouquet A 2005 Numerical study of dynamo action at low magnetic Prandtl numbers *Phys. Rev. Lett.* **94** 164502

[32] Minnini P D, Ponty Y, Montgomery D, Pinton J-F, Politano H and Pouquet A 2005 Nonlinear behaviour of a non-helical dynamo *Astrophys. J.* **626** 853

[33] Aumaitre S, Pétrélis F and Mallick K 2005 Low frequency noise controls on-off intermittency of bifurcating systems *Phys. Rev. Lett.* **95** 064101
Aumaitre S, Mallick K and Pétrélis F 2006 Effects of the low frequencies of noise on on-off-bifurcations *J. Stat. Phys.* **123** 909
Aumaitre S and Pétrélis F 2006 Modification of instability processes by multiplicative noises *Eur. J. Phys.* B **51** 357